ARTICLES

Structure of driven Alfvén waves with oblique magnetic field and dissipation

M. S. Ruderman[a] and A. N. Wright
School of Mathematical and Computational Sciences, St Andrews University, St Andrews, Fife KY16 9SS, Scotland, United Kingdom

(Received 21 September 1998; accepted 21 October 1998)

The quasi-resonant behavior of linear Alfvén waves in one-dimensional magnetized weakly resistive plasmas with the slightly inclined equilibrium magnetic field is studied. The analysis concentrates on the behavior of the *y*-component of the velocity, v, which is the component perpendicular both to the inhomogeneity direction and to the equilibrium magnetic field, and the *z*-component of the velocity, *w*, which is the component along the inhomogeneity direction. It is shown that the behavior of v and w is described by the functions $F(\sigma;\Lambda)$ and $G(\sigma;\Lambda)$, where σ is the dimensionless distance along the inhomogeneity direction and the parameter Λ characterizes the relative importance of resistivity and the magnetic field inclination near the quasi-resonant position. The functions $F(\sigma;\Lambda)$ and $G(\sigma;\Lambda)$ are generalizations of the F and G functions introduced by Goossens, Ruderman, and Hollweg [Sol. Phys. **157**, 75 (1995)] and coincide with them for $\Lambda=0$. The behavior of $F(\sigma;\Lambda)$ and $G(\sigma;\Lambda)$ is studied numerically for different values of Λ. It changes from monotonic to oscillatory when Λ is increased. It is shown that the connection formulas giving the jumps of *w* and the perturbation of the total pressure across the quasi-resonant layer and the rate of energy dissipation in the quasi-resonant layer are independent of the inclination angle. [S1070-664X(99)00703-X]

I. INTRODUCTION

One of the most interesting phenomena related to propagation of linear magnetohydrodynamic (MHD) waves in inhomogeneous plasmas is resonant coupling between global waves and local Alfvén or slow waves. In weakly dissipative plasmas, this resonant coupling occurs in thin resonant layers with the thickness determined by dissipative coefficients. The plasma motion in the resonant layers is characterized by large amplitudes and gradients. Resonant interaction of fast magnetosonic waves and Alfvén waves was suggested as a possible mechanism of excitation of ultra-low-frequency (ULF) MHD waves in the magnetosphere by Chen and Hasegawa[1] and Southwood.[2] Since these pioneering papers, this mechanism was remained popular for explaining excitation of ULF waves (see, e.g., Hughes[3] and Wright[4]).

Due to large gradients in resonant layers resonant MHD waves can be efficiently damped even in weakly dissipative plasmas. This property of resonant MHD waves inspired Ionson[5] to suggest resonant absorption of the wave energy in resonant layers as a possible mechanism of heating magnetic structures in the solar corona. Since this original work, resonant absorption has grown into a popular mechanism to explain solar coronal heating (see, e.g., Kuperus *et al.*,[6] Ionson,[7] Davila,[8] Hollweg,[9] and Goossens[10]). Recently, resonant absorption has been considered as a possible cause of the observed loss of power of acoustic oscillations in the vicinity of sunspots (Hollweg,[11] Lou,[12] Sakurai *et al.*,[13] Goossens and Poedts,[14] Goossens and Hollweg,[15] and Stenuit *et al.*[16]).

The theory of linear resonant MHD waves in inhomogeneous plasmas is extremely complicated when the equilibrium quantities depend on all spatial coordinates (e.g., Wright and Thompson[17] and references therein). The assumption that the equilibrium state depends on one spatial coordinate only results in a great simplification of the theory. In what follows we only consider the driven problem, where perturbations of all quantities harmonically oscillate with the frequency of the external driver. Then in the case of a one-dimensional equilibrium, the linear MHD equations can be Fourier analyzed with respect to time and two spatial coordinates. As a result, these equations are reduced to a set of ordinary differential equations. When the plasma is ideal, the one-dimensional equilibrium is planar, and the equilibrium magnetic field is unidirectional and perpendicular to the inhomogeneity direction, this set of equations contains a singular point. The solutions describing resonant MHD waves are singular at a resonant magnetic surface.

One-dimensional equilibria with the unidirectional magnetic field perpendicular to the direction of inhomogeneity are often used to model real magnetic configurations, such as the penumbral regions in the solar photosphere or the Earth's

[a]On leave of Institute for Problems in Mechanics, Russian Academy of Sciences, Moscow. Electronic mail: michaelr@dcs.st-and.ac.uk

magnetotail. However, the assumption that the equilibrium magnetic field is perpendicular to the inhomogeneity direction is highly unrealistic. In reality the magnetic field is only approximately perpendicular. The propagation of MHD waves in one-dimensional planar equilibria with the unidirectional oblique magnetic field was considered by Schwartz and Bel.[18] These authors showed that in the case of oblique magnetic field there is no singularity in the linear ideal MHD equations no matter how small the angle θ between the equilibrium magnetic field and the direction perpendicular to the inhomogeneity direction.

This result has an obvious physical interpretation. When θ is small (in particular, zero), strong transformation of the energy of a fast magnetosonic wave that carries energy across the magnetic surfaces into the energy of local Alfvén oscillations occurs in the vicinity of the quasi-resonant surface. Note that resonance occurs at a resonant magnetic surface when $\theta=0$. For $\theta\neq 0$, but $|\theta|\ll 1$, the resonant condition is satisfied only approximately and this approximate resonance occurs on a surface that is not a magnetic surface. We call this surface the ''quasi-resonant surface.'' When $\theta=0$, the energy of Alfvén oscillations is accumulated in the vicinity of the resonant magnetic surface because Alfvén waves cannot carry energy across the magnetic surfaces. Since in the driven problem we assume that the driving is acting for an infinitely long period of time, this energy accumulation results in the infinite wave amplitude at the resonant magnetic surface. On the other hand, when $\theta\neq 0$, the Alfvén waves carry the energy from the now quasi-resonant surface, so the wave amplitude is finite at the resonant position and the solution does not contain the singularity.

Inspired by Schwartz and Bel,[18] Goossens *et al.*[19] studied a more general situation where equilibrium quantities depend on two spatial variables. These authors showed that in this case once again there is the resonant magnetic surface and solutions describing driven MHD waves do contain the singularity. So one-dimensional equilibria with the oblique magnetic field are very exceptional from the point of view of the theory of resonant MHD waves in ideal plasmas.

Singularities in solutions describing resonant MHD waves appear because the approximation of ideal plasmas is used. Real plasmas are always dissipative. Dissipation removes singularities. However, when dissipation is small it is only important in a thin dissipative layer embracing the ideal resonant position. In the limit of very weak dissipation the amount of energy dissipated in the dissipative layer is independent of dissipative coefficients. As a result, the amount of dissipated energy can be correctly calculated even in the approximation of ideal plasma using the Landau rule to pass the singularity.

While real equilibria are always three-dimensional, one-dimensional equilibria very often give a good first approximation to reality. A better understanding of what happens when we pass from the case where $\theta=0$ to the case with $\theta\neq 0$ is very important for applications. Recently, this problem has become increasingly interesting for studying wave propagation in the Earth's magnetotail. Hansen and Harold[20] considered the energy deposition into a quasi-resonant layer in a cold, ideal, one-dimensional plasma with the slightly oblique unidirectional magnetic field ($|\theta|\ll 1$). These authors made wrong conclusions that the amount of energy dissipated in the quasi-resonant layer is independent of θ, and that the effect of finite θ is only important in the quasi-resonant layer embracing the resonant position that is present when $\theta=0$.

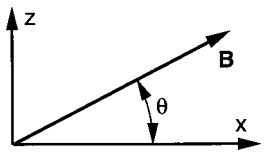

FIG. 1. The sketch of the equilibrium and coordinates. The magnetic field $\mathbf{B}=B(\cos\theta,0,\sin\theta)$ has constant strength. The density varies only with z, so if θ is nonzero there is a field-aligned density variation.

Later Wright and Garman[21] studied the same problem. These authors found strong mode conversion from the fast to Alfvén modes in the vicinity of a spatial quasi-resonant position corresponding to the Alfvén resonant position for $\theta=0$. However, they did not find any energy absorption, which is not surprising at all since the plasma was ideal and the solution nonsingular. The results by Wright and Garman[21] also show that, when $\theta\neq 0$, the solution differs from that for $\theta=0$ not only in the vicinity of the quasi-resonant position, but also in a very large domain beyond this position.

Hence, we have a peculiar situation. The energy absorption is identically zero when $\theta\neq 0$, while it is finite when $\theta=0$. Obviously, this situation arises from using the ideal plasma approximation. Actually, both $\theta\neq 0$ and dissipation remove the singularity in the linear MHD equations. So, from the physical point of view it is convenient to assume that there is at least some small dissipation and then to consider the limit $\theta\to 0$. In doing so we can hope to reconcile the two cases: $\theta\neq 0$ and $\theta=0$.

The aim of the present paper is to study the wave behavior in the quasi-resonant layer in a weakly dissipative plasma with the slightly oblique equilibrium magnetic field. The paper is organized as follows. In the next section we derive the linear governing equations for quasi-resonant waves. In Sec. III we obtain the solution to these equations describing the wave behavior in the quasi-resonant layer. In Sec. IV we use the solution obtained in Sec. III to study the wave behavior in the quasi-resonant layer. Section V contains summary and conclusions.

II. DERIVATION OF GOVERNING EQUATIONS

We consider a cold resistive plasma with the equilibrium density ρ depending on the z-coordinate only in the Cartesian coordinates x,y,z. The equilibrium magnetic field is constant and in the xz-plane, so that it can be written as

$$\mathbf{B}=B(\cos\theta,0,\sin\theta) \tag{1}$$

with θ the angle between the equilibrium magnetic field and the x-axis (see Fig. 1). We choose such a direction of the x-axis that $\theta>0$. The linear momentum and induction equations take the form

$$\rho\frac{\partial \mathbf{v}}{\partial t}=-\nabla P+\frac{1}{\mu}(\mathbf{B}\cdot\nabla)\mathbf{b}, \tag{2}$$

$$\frac{\partial \mathbf{b}}{\partial t}=(\mathbf{B}\cdot\nabla)\mathbf{v}-\mathbf{B}\nabla\cdot\mathbf{v}+\eta\nabla^2\mathbf{b}. \tag{3}$$

Here $\mathbf{v}=(u,v,w)$ is the velocity, $\mathbf{b}=(b_x,b_y,b_z)$ is the perturbation of the magnetic field, μ is the magnetic permiability of vacuum, and η is the coefficient of magnetic field diffusion. P is the perturbation of the magnetic pressure given by

$$P=\frac{1}{\mu}(\mathbf{B}\cdot\mathbf{b}). \tag{4}$$

In what follows, we assume that the magnetic Reynolds number is very large. This assumption enables us to use results obtained on the basis of ideal MHD when calculating the last term on the right-hand side of Eq. (3). As a result we arrive at

$$\frac{\partial^2 \mathbf{b}}{\partial t^2}=(\mathbf{B}\cdot\nabla)\frac{\partial \mathbf{v}}{\partial t}-\mathbf{B}\nabla\cdot\frac{\partial \mathbf{v}}{\partial t}+\eta\nabla^2[(\mathbf{B}\cdot\nabla)\mathbf{v}-\mathbf{B}\nabla\cdot\mathbf{v}]. \tag{5}$$

Eliminating $\mathbf{b}$ from Eqs. (2) and (5) we obtain

$$\rho\frac{\partial^3 \mathbf{v}}{\partial t^3}=-\nabla\frac{\partial^2 P}{\partial t^2}+\frac{1}{\mu}(\mathbf{B}\cdot\nabla)\left(\frac{\partial}{\partial t}+\eta\nabla^2\right)[(\mathbf{B}\cdot\nabla)\mathbf{v}-\mathbf{B}\nabla\cdot\mathbf{v}]. \tag{6}$$

The y-component of this equation is

$$\rho\frac{\partial^3 v}{\partial t^3}-\frac{1}{\mu}(\mathbf{B}\cdot\nabla)^2\left(\frac{\partial v}{\partial t}+\eta\nabla^2 v\right)=-\frac{\partial^3 P}{\partial t^2\partial y}. \tag{7}$$

It follows from Eq. (2) that

$$\mathbf{B}\cdot\mathbf{v}=0. \tag{8}$$

Taking the scalar product of Eq. (3) with $\mathbf{B}$ we obtain

$$\frac{1}{\mu}B^2\nabla\cdot\mathbf{v}=-\frac{\partial P}{\partial t}+\eta\nabla^2 P. \tag{9}$$

Elimination of u and v from Eqs. (7)–(9) yields

$$\left[\frac{\partial^3}{\partial t^3}-\frac{(\mathbf{B}\cdot\nabla)^2}{\mu\rho}\left(\frac{\partial}{\partial t}+\eta\nabla^2\right)\right]\left[\rho v_A^2\left(\frac{\partial w}{\partial z}-\frac{\partial w}{\partial x}\tan\theta\right)+\frac{\partial P}{\partial t}-\eta\nabla^2 P\right]=v_A^2\frac{\partial^4 P}{\partial t^2\partial y^2}, \tag{10}$$

where $v_A^2=B^2/\mu\rho$. We take the z-component of Eq. (6) and use Eq. (9) to get

$$\frac{\partial^3 P}{\partial t^2\partial z}-\frac{\sin\theta}{B}(\mathbf{B}\cdot\nabla)\left(\frac{\partial^2 P}{\partial t^2}-\eta^2\nabla^4 P\right)=-\rho\frac{\partial^3 w}{\partial t^3}+\frac{1}{\mu}(\mathbf{B}\cdot\nabla)^2\left(\frac{\partial w}{\partial t}+\eta\nabla^2 w\right). \tag{11}$$

Equations (10) and (11) constitute the set of equations for w and P.

Now we study the steady state of driven oscillations where all quantities oscillate with a real positive frequency ω. Since the equilibrium state is independent of x and y, we can Fourier analyze perturbations with respect to this variable. This consideration enables us to take perturbations of all quantities proportional to $\exp[i(k_x x+k_y y-\omega t)]$. Then Eqs. (7), (10), and (11) are transformed to

$$\omega^2 v+v_A^2\left(\sin\theta\frac{d}{dz}+ik_x\cos\theta\right)^2\left(v+\frac{i\eta}{\omega}\frac{d^2 v}{dz^2}\right)=\frac{\omega k_y}{\rho}P, \tag{12}$$

$$\left[\omega^2+v_A^2\left(\sin\theta\frac{d}{dz}+ik_x\cos\theta\right)^2\left(1+\frac{i\eta}{\omega}\frac{d^2}{dz^2}\right)\right]\times\left[\rho v_A^2\left(\frac{dw}{dz}-ik_x w\tan\theta\right)-i\omega P-\eta\frac{d^2 P}{dz^2}\right]=-i\omega v_A^2 k_y^2 P, \tag{13}$$

$$\frac{dP}{dz}-\sin\theta\left(\sin\theta\frac{d}{dz}+ik_x\cos\theta\right)\left(P+\frac{\eta^2}{\omega^2}\frac{d^4 P}{dz^4}\right)=i\rho\omega w+\frac{i\rho v_A^2}{\omega}\left(\sin\theta\frac{d}{dz}+ik_x\cos\theta\right)^2\left(w+\frac{i\eta}{w}\frac{d^2 w}{dz^2}\right). \tag{14}$$

When deriving these equations we have used the fact that resistivity is only important in the thin dissipative layer where the characteristic scale in the z-direction is much smaller than those in the x- and y-directions. This fact has enabled us to use the approximation $\eta\nabla^2\approx\eta d^2/dz^2$.

Equations (12)–(14) will be used in the next sections to obtain the solution describing the wave behavior in a quasi-resonant dissipative layer.

III. SOLUTION IN THE DISSIPATIVE LAYER

In what follows we restrict our analysis to the case where the magnetic field is quasi-horizontal, i.e., $\theta\ll 1$. This assumption enables us to use the approximation $\sin\theta\approx\theta$, $\cos\theta\approx 1$. Then Eqs. (12)–(14) take the form

$$\theta^2\frac{d^2 v}{dz^2}+2ik_x\theta\frac{dv}{dz}+\frac{\omega^2-v_A^2k_x^2}{v_A^2}v+\frac{i\eta}{\omega}\left(\theta\frac{d}{dz}+ik_x\right)^2\frac{d^2 v}{dz^2}=\frac{\omega k_y}{\rho v_A^2}P, \tag{15}$$

$$\theta^2\frac{d^3 w}{dz^3}+2ik_x\theta\frac{d^2 w}{dz^2}+\frac{\omega^2-v_A^2k_x^2}{v_A^2}\frac{dw}{dz}+\frac{i\eta}{\omega}\left(\theta\frac{d}{dz}+ik_x\right)^2\frac{d^3 w}{dz^3}=\frac{i\omega(\omega^2-v_A^2k^2)}{\rho v_A^4}P+\frac{i\omega\theta^2}{\rho v_A^2}\frac{d^2 P}{dz^2}-\frac{2\omega k_x\theta}{\rho v_A^2}\frac{dP}{dz}+\frac{\eta\omega^2}{\rho v_A^4}\times\left[1+\frac{i\eta v_A^2}{\omega^3}\left(\theta\frac{d}{dz}+ik_x\right)^2\frac{d^2}{dz^2}\right]\frac{d^2 P}{dz^2}, \tag{16}$$

$$\frac{dP}{dz}-\frac{\theta\eta^2}{\omega^2}\left(\theta\frac{d}{dz}+ik_x\right)\frac{d^4P}{dz^4}$$
$$=i\rho\omega w+\frac{i\rho v_A^2}{\omega}\left(\theta\frac{d}{dz}+ik_x\right)^2\left(w+\frac{i\eta}{\omega}\frac{d^2w}{dz^2}\right). \quad (17)$$

When deriving these equations, we have neglected obviously small terms like, e.g., $\theta^2 dP/dz$ on the left-hand side of Eq. (17) or $ik_x\theta(\omega^2/v_A^2-k_x^2)w$ on the left-hand side of Eq. (16).

When $\theta=0$ and $\eta=0$ Eqs. (15)–(17) are reduced to

$$\rho(\omega^2-v_A^2k_x^2)v=\omega k_y P, \quad (18)$$

$$\rho v_A^2(\omega^2-v_A^2k_x^2)\frac{dw}{dz}=i\omega(\omega^2-v_A^2k^2)P, \quad (19)$$

$$\omega\frac{dP}{dz}=i\rho(\omega^2-v_A^2k_x^2)w. \quad (20)$$

The solution to these equations is singular at the Alfvén resonant position z_A determined by the equation

$$v_A(z_A)=\frac{\omega}{|k_x|}. \quad (21)$$

It is straightforward to show that in the vicinity of z_A this solution is given by

$$P=\text{const}, \quad v=\frac{\omega k_y P}{\rho\Delta(z-z_A)}, \quad (22)$$

$$w=-\frac{i\omega k_y^2 P}{\rho\Delta}\ln|z-z_A|+\text{const}. \quad (23)$$

When deriving Eqs. (22) and (23), we have used the Taylor expansion

$$\omega^2-v_A^2k_x^2=\Delta(z-z_A), \quad \Delta=-k_x^2\left.\frac{dv_A^2}{dz}\right|_{z=z_A}. \quad (24)$$

This expansion is valid in the interval $[z_A-s,z_A+s]$ with s much smaller than the characteristic scale of the density variation l_{eq}.

Including the magnetic field inclination and/or resistivity removes the Alfvén singularity. We assume *ad hoc* that the both effects are only important in a thin resonant layer embracing z_A. We shall check this *ad hoc* assumption after we obtain the solution in the quasi-resonant layer. Actually, we can consider two, in general, different characteristic scales in this layer. The first scale is the resistive scale δ_A. We obtain it comparing the third and fourth terms on the left-hand side of Eq. (15) or (16). As a result we have

$$\delta_A=\left|\frac{\omega\eta}{\Delta}\right|^{1/3}. \quad (25)$$

The second scale is the inclination scale δ_θ. We obtain it comparing the second and third terms on the left-hand side of Eq. (15) or (16). The result is

$$\delta_\theta=\left|\frac{\theta\omega^2}{k_x\Delta}\right|^{1/2}=|\Lambda|^{1/2}\delta_A, \quad \Lambda=\frac{\theta}{k_x}\left|\frac{\omega^4}{\eta^2\Delta}\right|^{1/3}. \quad (26)$$

Since $\theta\geqslant 0$ the sign of Λ coinsides with the sign of k_x.

When $|\Lambda|\ll 1$ it is straightforward to see that the resistive terms on the left-hand sides of Eqs. (15) and (16) dominate the first and second terms and $|\theta df/dz|\ll|k_x f|$, where f is either v or w. Therefore, the first and second terms can be neglected in comparison with the fourth terms and in the latter $\theta d/dz$ can be neglected in comparison with ik_x.

In what follows we assume that $|k_x|l_{\text{eq}}=\mathcal{O}(1)$. When $|\Lambda|\gtrsim 1$, the second terms on the left-hand sides of Eqs. (15) and (16) are of the order of larger than the fourth terms. However, the ratio of the first terms to the second terms are of the order $|\theta|^{1/2}\ll 1$, so that the first terms can be neglected. It is straightforward to show that the ratio of $\theta df/dz$ to $|k_x f|$ is of the order $|\theta/k_x l_{\text{eq}}|^{1/2}\sim\theta^{1/2}\ll 1$. Hence, for any value of Λ we can simplify Eq. (15) to

$$\Delta(z-z_A)v+\frac{2i\omega^2\theta}{k_x}\frac{dv}{dz}-i\eta\omega\frac{d^2v}{dz^2}=\frac{\omega k_y}{\rho}P. \quad (27)$$

We cannot neglect the resistive term even when $\Lambda\gg 1$ because this is the only term providing dissipation.

The left-hand side of Eq. (16) can be rewritten in the same simplified form as the left-hand side of Eq. (27). However, before writing down the simplified version of Eq. (16), we consider its right-hand side. Simple estimates show that the first term on the right-hand side is much larger that all other terms. In addition, due to the resonant condition (21) we can use the approximation $\omega^2-v_A^2k^2\approx -v_A^2k_y^2$. As a result, the simplified form of Eq. (16) is

$$\Delta(z-z_A)\frac{dw}{dz}+\frac{2i\omega^2\theta}{k_x}\frac{d^2w}{dz^2}-i\eta\omega\frac{d^3w}{dz^3}=\frac{i\omega k_y^2}{\rho}P. \quad (28)$$

It is straightforward to show that the ratios of all terms in Eq. (17) to the first term on the left-hand side are small. This observation leads to the approximate equation $dP/dz\approx 0$, or

$$P=\text{const}. \quad (29)$$

Hence, the right-hand sides of Eqs. (27) and (28) are constant.

It is convenient to introduce the new dimensionless variable $\sigma=(z-z_A)/\delta_A$. Then we rewrite Eqs. (27) and (28) as

$$\frac{d^2v}{d\sigma^2}-2\Lambda\frac{dv}{d\sigma}+i\sigma v\,\text{sign}\,\Delta=\frac{i\omega k_y}{\rho|\Delta|\delta_A}P, \quad (30)$$

$$\frac{d^3w}{d\sigma^3}-2\Lambda\frac{d^2w}{d\sigma^2}+i\sigma\,\text{sign}\,\Delta\frac{dw}{d\sigma}=\frac{\omega k_y}{\rho|\Delta|}P. \quad (31)$$

To solve these equations we follow Ruderman *et al.*[22] and Tirry and Goossens[23] and introduce the Fourier transform with respect to σ,

$$\hat{f}(s)=\int_{-\infty}^{\infty}f(\sigma)e^{-i\sigma s}d\sigma. \quad (32)$$

Applying this transform to Eq. (30), we obtain

$$\frac{d\hat{v}}{ds}+\text{sign}\,\Delta(2i\Lambda s+s^2)\hat{v}=-\frac{2\pi i\omega k_y P}{\rho\Delta\delta_A}\delta(s). \quad (33)$$

The solution to this equation vanishing as $|s|\to\infty$ is

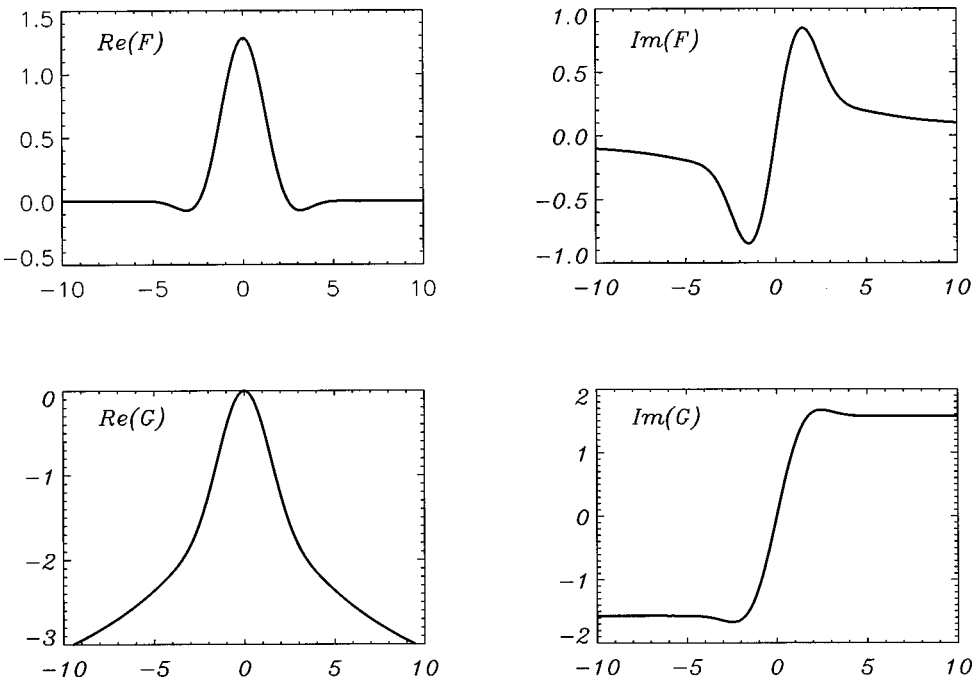

FIG. 2. The real and imaginary parts of the functions $F(\sigma;\Lambda)$ and $G(\sigma;\Lambda)$ versus dimensionless coordinate σ across the quasi-resonant layer for $\Lambda=0$.

$$\hat{v}=-\frac{\pi i\omega k_y P}{\rho|\Delta|\delta_A}[1+\mathrm{sign}(\Delta s)]\times\exp\left[-\mathrm{sign}\,\Delta\left(i\Lambda s^2+\frac{1}{3}s^3\right)\right]. \tag{34}$$

Then the inverse Fourier transform yields

$$v=-\frac{i\omega k_y P}{\rho|\Delta|\delta_A}F(\sigma;\Lambda), \tag{35}$$

where the F-function is given by

$$F(\sigma;\Lambda)=\int_0^\infty \exp[i(\sigma s-\Lambda s^2)\mathrm{sign}\,\Delta-\tfrac{1}{3}s^3]ds. \tag{36}$$

The expression for $dw/d\sigma$ is obtained by substitution of $\omega k_y^2 P/\rho|\Delta|$ for $i\omega k_y P/\rho|\Delta|\delta_A$ in Eq. (35). We then integrate this expression to arrive at

$$w=\frac{i\omega k_y^2 P}{\rho\Delta}G(\sigma;\Lambda)+\mathrm{const}, \tag{37}$$

with the G-function given by

$$G(\sigma;\Lambda)=\int_0^\infty \frac{e^{i\sigma s\ \mathrm{sign}\,\Delta}-1}{s}\times\exp(-i\Lambda s^2\,\mathrm{sign}\,\Delta-\tfrac{1}{3}s^3)ds. \tag{38}$$

When $\Lambda=0$, the functions $F(\sigma;\Lambda)$ and $G(\sigma;\Lambda)$ coincide with the functions $F(\sigma)$ and $G(\sigma)$ first introduced by Boris,[24] and then used by Mok and Einaudi[25] and Goossens *et al.*[26] to describe resonant MHD waves in dissipative layers (see also the review paper by Goossens and Ruderman[27]). In the next section we use Eqs. (35)–(38) to study the dependence of the behavior of resonant Alfvén waves in the quasi-resonant layer on the inclination parameter Λ.

IV. WAVE BEHAVIOR IN THE QUASI-RESONANT LAYER

When $\theta=0$, ideal MHD predicts that v and b_y have $1/(z-z_A)$ singularities in the vicinity of the resonant position, w and b_z have logarithmic singularities, and all other quantities are regular. In what follows we concentrate on quantities that are singular in ideal MHD when $\theta=0$. It can be shown that b_y is proportional to v, and b_z is proportional to w. Hence it is enough to study the behavior of v and w only. Since, in accordance with Eqs. (35) and (37), the behavior of these quantities is determined by the the functions $F(\sigma;\Lambda)$ and $G(\sigma;\Lambda)$, in this section we study the behavior of these functions. In Figs. 2–4 the dependencies of the real and imaginary parts of $F(\sigma;\Lambda)$ and $G(\sigma;\Lambda)$ on σ are shown for $\Lambda=0$, $\Lambda=3$ and $\Lambda=15$, respectively. As it has been noted, for $\Lambda=0$ $F(\sigma;\Lambda)$ and $G(\sigma;\Lambda)$ coincide with the F and G functions in Goossens *et al.*[26] Correspondingly, Fig. 2 coincides with Figs. 1 and 2 in Goossens *et al.*[26] In Figs. 2–4 we see the transition from the monotonic behavior of the wave amplitude in the quasi-resonant layer for $\Lambda=0$ to the oscillatory behavior for $\Lambda=15$. Since the function $F(\sigma;\Lambda)$ determines the behavior of the most singular quantity v, corresponding to the Alfvén waves, we calculated in Appendix B its asymptotic behavior for $\Lambda\to\infty$. The dotted lines in Fig. 4 show the real and imaginary parts of $F(\sigma;\Lambda)$ given by asymptotic formulas (66) and (68). There is some difference between asymptotic and exact results for large positive values of σ where the wave amplitude is small anyway. However, for moderate positive values of σ and for all negative values, coincidence of the asymptotic and the exact results is excellent, so the solid and dotted curves are indistinguishable for these values of σ.

In accordance with Eq. (71), for large values of Λ, the amplitude of oscillations near the quasi-resonant position z_A

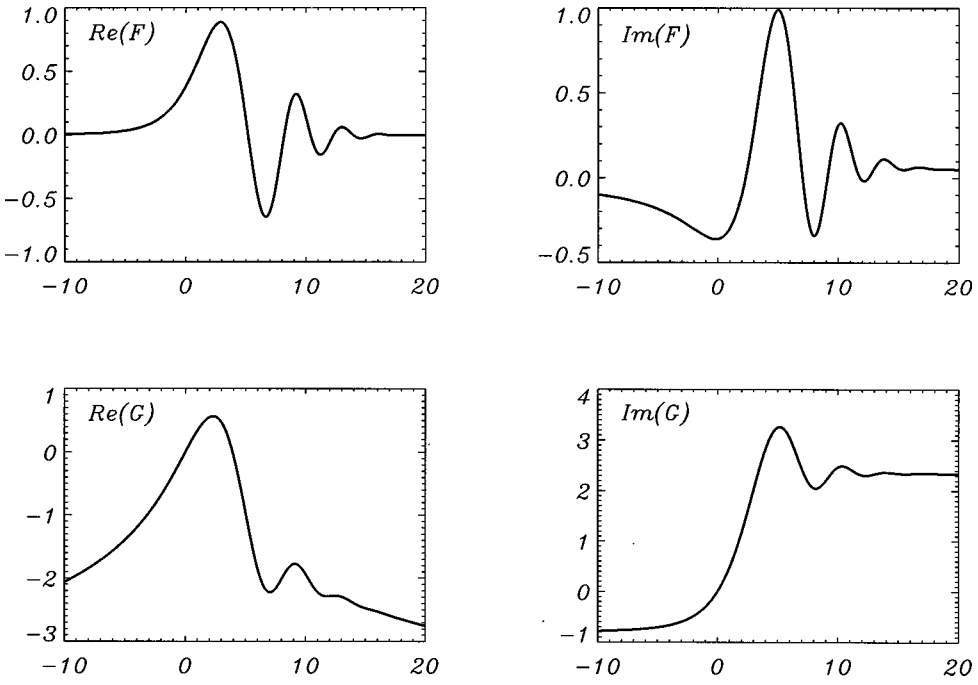

FIG. 3. The same as Fig. 2, however for $\Lambda=3$.

decays as $\Lambda^{-1/2}$ when Λ is increased. The resonant layer can be divided into the left part ($z<z_A$) and the right part ($z>z_A$). In the left part, the amplitude behaves monotonically and reaches its asymptotic behavior $(z-z_A)^{-1}$ at the distance of the order $\Lambda^{1/2}\delta_A$. So, the thickness of the left part is of the order $\Lambda^{1/2}\delta_A$. In the right part, the behavior of the wave amplitude is oscillatory with the characteristic oscillation period of the order $\Lambda^{1/2}\delta_A$. The amplitude of oscillations exponentially decreases with the distance from z_A on the scale of the order $\Lambda\delta_A$. At the distances of the order of a few $\Lambda\delta_A$, the wave amplitude reaches its asymptotic behavior $(z-z_A)^{-1}$, so the quantity $\Lambda\delta_A$ can be taken as the thickness of the right part of the quasi-resonant layer. Since the thickness of the right part is much larger than that of the left part, the quantity $\Lambda\delta_A$ can also be taken as the thickness of the whole dissipative layer. It is interesting to note that, in accordance with Eq. (26), the quantity $\Lambda^{1/2}\delta_A$ equals δ_θ, which is independent of the coefficient of magnetic diffusion η, while $\Lambda\delta_A$ is proportional to $\eta^{-1/3}$. Hence, for large Λ (i.e., small η) the characteristic period of oscillations of the wave amplitude in the quasi-resonant layer is independent of η, while the thickness of the resonant layer is proportional to $\eta^{-1/3}$. The latter result is in contrast with the corresponding result for the thickness of the resonant layer in the case θ

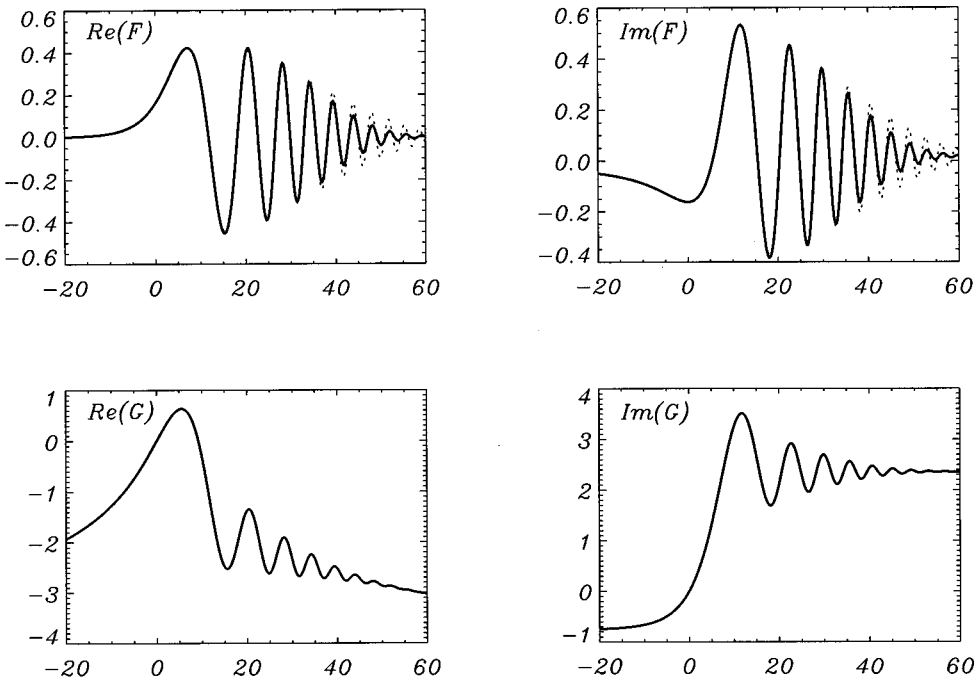

FIG. 4. The same as Fig. 2, however for $\Lambda=15$. The dotted lines in the upper panels show the asymptotical approximation for $F(\sigma;\Lambda)$.

$=0$, where this thickness is proportional to $\eta^{1/3}$ (e.g., Goossens *et al.*[26]).

Now we can discuss the *ad hoc* assumption made in Sec. III that the thickness of the quasi-resonant layer is much smaller than the characteristic scale of inhomogeneity $l_{\rm eq}$. When $\theta=0$ this assumption is reduced to $\delta_A \ll l_{\rm eq}$ and, since $\delta_A \sim \eta^{1/3}$, it is always satisfied for the large values of the magnetic Reynolds number R_m. However, when $\theta \neq 0$, the situation is more complicated. When R_m is very large, the characteristic thickness of the quasi-resonant layer is $\Lambda \delta_A$, so we obtain the restriction $\Lambda \delta_A \ll l_{\rm eq}$. Together with the demand that R_m be large, it gives

$$1 \ll \mathrm{R}_m^{1/3} \ll \theta^{-1}. \tag{39}$$

When deriving this condition, we have used the estimate $|\Delta| \sim \omega^2 / l_{\rm eq}$ and assumed that $|k_x| l_{\rm eq} \sim 1$. For instance, in the solar photosphere typically $\mathrm{R}_m \sim 10^6$, and restriction (39) is satisfied only for $\theta \ll 1°$.

It is instructive to compare Fig. 4 with Figs. 4 and 5 by Wright and Garman[21] showing the picture of transformation of the incoming fast wave into the outgoing Alfvén wave. The two upper panels of our Fig. 4 qualitatively coincide with the upper panels of Figs. 4 and 5 by Wright and Garman[21] except their left regions far from the quasi-resonant position where there is an incoming wave.

As we have seen there is strong qualitative difference in the behavior of the quasi-resonant waves in the two cases: $\Lambda \lesssim 1$ and $\Lambda \gg 1$. However, we have found this difference studying the problem from the ''inner'' point of view, i.e., when we are interested in the wave behavior in the quasi-resonant layer. There is also the 'outer' point of view. This point of view is most completely expressed in the concept of connection formulas first introduced by Sakurai *et al.*[28] and then further developed by Goossens *et al.*[26] and Goossens and Ruderman.[27] This concept can be described as follows. Let us assume that the quasi-resonant layer embracing the quasi-resonant position is thin in comparison with the characteristic scale of the problem (e.g., wavelength). Then we can use the method of matched asymptotic expansions to describe the resonant wave. In accordance with this method, we obtain the inner solution to the problem, which is the solution in the quasi-resonant layer, and the outer solution, which is the solution to the left and the right to the quasi-resonant layer and far enough from the quasi-resonant position. Then we match the two solutions in the two overlap regions to the left and the right to the quasi-resonant layer, where both the inner and the outer solutions are valid.

Since we consider a weakly dissipative plasma, dissipation is important only in the quasi-resonant layer. The outer solution can be obtained on the basis of ideal MHD. For a one-dimensional equilibrium state, the linear ideal MHD equations can be reduced to two equations for w and P. When solving the outer problem, we can consider the quasi-resonant layer as a surface of discontinuity. Then the only quantities we need to solve the outer problem are the jumps in the quantities w and P across the quasi-resonant layer, $[w]$ and $[P]$. The expressions for $[w]$ and $[P]$ are called the connection formulas. In accordance with Eq. (29), $[P]=0$. Using Eq. (37) and Eq. (A6) from Appendix A we obtain

$$[w] = \lim_{\sigma \to \infty} \{w(\sigma) - w(-\sigma)\} = -\frac{\pi \omega k_y^2 P}{\rho |\Delta|}. \tag{40}$$

The remarkable property of this second connection formula is that $[w]$ is independent of η and θ. Hence, from the ''outer'' point of view the two cases, $\Lambda \lesssim 1$ and $\Lambda \gg 1$, are absolutely indistinguishable.

Let us show that the amount of energy dissipated in the quasi-resonant layer over one period is independent of η and θ. Wright and Allan[29] showed that the amount of energy dissipated in a resonant layer per wave period in the x- and y-directions is proportional to $\int_{-\infty}^{\infty} |dF/d\sigma|^2 d\sigma$ with the proportionality coefficient independent of η. These authors considered the case $\theta=0$, however, it is straighforward to check that their calculations are also valid for $\theta \neq 0$. The coefficient of proportionality is now independent of both η and θ. Therefore, to show that the amount of energy dissipated in the quasi-resonant layer is independent of η and θ, it is enough to show that $\int_{-\infty}^{\infty} |dF/d\sigma|^2 d\sigma$ is independent of Λ. Using the Parseval identity, we obtain

$$\int_{-\infty}^{\infty} \left| \frac{dF}{d\sigma} \right|^2 d\sigma = \frac{1}{2\pi} \int_{-\infty}^{\infty} s^2 |\hat{F}(s;\Lambda)|^2 ds. \tag{41}$$

In accordance with Eqs. (34) and (35)

$$\hat{F}(s;\Lambda) = \pi [1 + \mathrm{sign}(\Delta s)] \exp[-\mathrm{sign}\,\Delta (i\Lambda s^2 + \tfrac{1}{3} s^3)]. \tag{42}$$

Substituting Eq. (42) into Eq. (41) we immediately arrive at

$$\int_{-\infty}^{\infty} \left| \frac{dF}{d\sigma} \right|^2 d\sigma = \pi. \tag{43}$$

Independence of the energy dissipated in the quasi-resonant layer on θ is exactly what was claimed by Hansen and Harrold.[20] However, they also claimed that their result was obtained on the basis of linear ideal MHD, which must be wrong because energy cannot be dissipated in ideal plasmas.

V. SUMMARY AND CONCLUSIONS

In this paper we studied the structure of linear Alfvén waves in quasi-resonant layers. We assumed that the equilibrium state is one-dimensional with the magnetic field inclined with respect to the direction of inhomogeneity. The angle θ between the direction perpendicular to the inhomogeneity direction and the equilibrium magnetic field was assumed to be small. The only dissipative process taken into account was finite resistivity. It was assumed that the coefficient of magnetic diffusion η was small, i.e., that the magnetic Reynolds number was large. Since $\theta \neq 0$, there was no exact Alfvén resonance. However, due to the assumption that $\theta \ll 1$, there was a quasi-resonant position z_A where the Alfvén resonant condition is approximately satisfied and efficient coupling of fast and Alfvén waves occurs.

We showed that the perturbation of the total pressure does not vary across the quasi-resonant layer embracing z_A. This result coincides with the similar result obtained previously for resonant layers in case $\theta=0$. We studied the be-

havior of the y- and z-components of the velocity, v and w, in the quasi-resonant layer. We showed that the behavior of these quantities is decribed by the functions $F(\sigma;\Lambda)$ and $G(\sigma;\Lambda)$, where σ is the dimensionless distance across the quasi-resonant layer and Λ characterizes the relative importance of resistivity and the magnetic field inclination. The functions $F(\sigma;\Lambda)$ and $G(\sigma;\Lambda)$ are the generalizations of the F and G functions introduced by Goossens *et al.*[26] and coincide with them when $\Lambda=0$.

We studied the behavior of $F(\sigma;\Lambda)$ and $G(\sigma;\Lambda)$ for different values of the parameter Λ. This behavior changes from monotonic to oscillatory when Λ is increased. We obtain asymptotic formulas for $F(\sigma;\Lambda)$ and $G(\sigma;\Lambda)$ valid for $\Lambda \gg 1$. Comparison of these formulas with the exact numerical results for $\Lambda=15$ shows that the asymptotic formulas give an excellent description of $F(\sigma;\Lambda)$ except in the region $\sigma \gtrsim \Lambda$, where the wave amplitudes are small anyway. For large values of Λ the period of the amplitude oscillation in the quasi-resonant layer is of the order $\Lambda^{1/2}\delta_A$ and is independent of η, and the thickness of the quasi-resonant layer is of the order $\Lambda\delta_A$ and is proportional to $\eta^{-1/3}$, where δ_A is the thickness of the dissipative layer when $\theta=0$. This result is in contrast to the corresponding result for the case $\theta=0$, where the thickness of the resonant layer is proportional to $\eta^{1/3}$.

We obtained connection formulas giving the jump in the quantities P and w across the quasi-resonant layer, $[P]$ and $[w]$. We showed that $[P]=0$ and $[w]$ is given by the same expression as in case $\theta=0$. We showed that the rate of wave energy dissipation in the quasi-resonant layer is also independent of Λ.

ACKNOWLEDGMENTS

M.R. acknowledges support from PPARC (Particle Physics and Astronomy Research Council). A.W. is supported by a PPARC Advanced Fellowship.

APPENDIX A: ASYMPTOTIC BEHAVIOR OF FUNCTIONS $F(\sigma;\Lambda)$ AND $G(\sigma;\Lambda)$ FOR LARGE $|\sigma|$

Let us study the asymptotic behavior of the functions $F(\sigma;\Lambda)$ and $G(\sigma;\Lambda)$ for $|\sigma|\to\infty$. Integration by parts in Eq. (36) immediately gives

$$F(\sigma;\Lambda)\simeq i\sigma^{-1}. \tag{A1}$$

Now we proceed to the function $G(\sigma;\Lambda)$. We rewrite Eq. (38), determining this function as

$$G(\sigma;\Lambda)=G(\sigma;0)+I(\sigma;\Lambda)+J(\Lambda), \tag{A2}$$

where

$$I(\sigma;\Lambda)=\int_0^\infty \exp(i\sigma s\,\mathrm{sign}\,\Delta-\tfrac{1}{3}s^3) \times[\exp(-i\Lambda s^2\,\mathrm{sign}\,\Delta)-1]\frac{ds}{s}, \tag{A3}$$

$$J(\Lambda)=\int_0^\infty [1-\exp(-i\Lambda s^2\,\mathrm{sign}\,\Delta)]e^{-s^3/3}\frac{ds}{s}. \tag{A4}$$

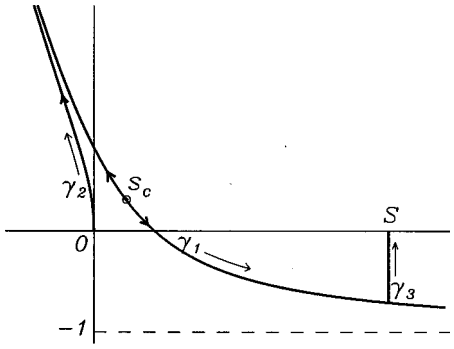

FIG. 5. The picture of the contours of the constant phase (γ_1 and γ_2) for $\kappa>0$. The contour γ_3 is auxiliary. The point s_c is the stationary point. The dashed line is an asymptote for the contour γ_1. The arrows on the contours γ_1 and γ_2 show the directions of the steepest descent. The arrows near the contours show the direction of integration.

We use integration by parts to obtain

$$I(\sigma;\Lambda)\simeq i\Lambda\sigma^{-2}\,\mathrm{sign}\,\Delta. \tag{A5}$$

Then it follows from Eqs. (A2) and (A5) and the asymptotic expansion of $G(\sigma;0)$ for large σ (see, e.g., Goossens *et al.*,[26] equation 95) that

$$G(\sigma;\Lambda)\simeq -\ln|\sigma|-\tfrac{2}{3}C-\tfrac{1}{3}\ln 3+J(\Lambda)+\tfrac{1}{2}\pi i\,\mathrm{sign}(\sigma\Lambda), \tag{A6}$$

where $C\approx 0.5722$ is the Euler–Masceroni constant. It is straightforward to see that $J(0)=0$.

When $|\Lambda|\lesssim 1$, asymptotic formulas (A1) and (A6) are valid for $|\sigma|\gg 1$. However, for $\Lambda\gg 1$ the applicability conditions are different. They will be discussed in Appendix B.

APPENDIX B: ASYMPTOTIC BEHAVIOR OF FUNCTION $F(\sigma;\Lambda)$ FOR LARGE Λ

In this Appendix we study the asymptotic behavior of the function $F(\sigma;\Lambda)$ for $|\Lambda|\to\infty$. Since changing the sign of Δ results in the substitution of $F(\sigma;\Lambda)$ by the complex conjugate quantity $F^*(\sigma;\Lambda)$, we assume that $\Delta>0$. The relation $F(-\sigma;-\Lambda)=F^*(\sigma;\Lambda)$ enables us to take $\Lambda>0$. To evaluate the asymptotic behaviour we use the method of the steepest discent (see, e.g., Nayfeh,[30] and Bender and Orszag[31]). We shall see in what follows that the analysis strongly depends on the sign of σ. Therefore, we study the two cases, $\sigma>0$ and $\sigma<0$, separately.

(i) $\sigma>0$. We make the substitution $s'=\Lambda s$ and drop the prime to rewrite Eq. (36) as

$$F(\sigma;\Lambda)=\Lambda\int_0^\infty \exp[\Lambda^3 h(s)]ds \tag{B1}$$

with

$$h(s)=i(\kappa s-s^2)-\tfrac{1}{3}s^3,\quad \kappa=\sigma\Lambda^{-2}. \tag{B2}$$

In what follows we assume that $\kappa\lesssim 1$, i.e., $\sigma\lesssim\Lambda^2$. The function $h(s)$ has a critical point s_c given by

$$s_c=-i+(i\kappa-1)^{1/2}, \tag{B3}$$

where we take the branch of the square root with the positive real part. The contours of the stationary phase passing

throuth the stationary point s_c, γ_1, and through the origin of the coordinates, γ_2, are shown in Fig. 5. The arrows on these contours show the directions of the steepest descent. Since $h(s)$ is an analytical function, we obtain

$$\int_0^S \exp[\Lambda^3 h(s)]ds = \left(\int_{\gamma_1^S} + \int_{\gamma_2} + \int_{\gamma_3} \right) \exp[\Lambda^3 h(s)]ds, \tag{B4}$$

where the contour γ_3 is the straight vertical segment connecting the contour γ_1 and the point S on the real axis, and γ_1^S is the part of the contour γ_1 restricted by this segment (see Fig. 5). The arrows near the contours γ_1, γ_2, and γ_3 show the direction of integration. It is straightforward to show that the horizontal line determined by the equation $\Im(s) = -1$ ($\Im$ indicates the imaginary part) is the asymptote of the contour γ_1. It is shown by the dashed line in Fig. 5. Hence, the length of the segment γ_3 tends to 1 when $S \to \infty$. On the other hand, it is easy to see that $\Re[h(s)] \to -\infty$ *as* $S \to \infty$ ($\Re$ indicates the real part). Therefore

$$\int_{\gamma_3} \exp[\Lambda^3 h(s)]ds \to 0 \quad \text{as} \quad S \to \infty, \tag{B5}$$

and we arrive at

$$\int_0^\infty \exp[\Lambda^3 h(s)] = I_1(\Lambda) + I_2(\Lambda), \tag{B6}$$

where

$$I_1(\Lambda) = \int_{\gamma_1} \exp[\Lambda^3 h(s)]ds, \tag{B7}$$

$$I_2(\Lambda) = \int_{\gamma_2} \exp[\Lambda^3 h(s)]ds. \tag{B8}$$

When $\Lambda \to \infty$, the main contributions to the integrals on γ_1 and γ_2 are given by the immediate vicinities of s_c and the origin of the coordinates, respectively. In these vicinities the function $h(s)$ can be approximated by

$$h(s) \approx \tfrac{1}{3}[3\kappa + 2i + 2(i\kappa - 1)^{3/2}] - (i\kappa - 1)^{1/2}(s - s_c)^2 \tag{B9}$$

and by

$$h(s) \approx i\kappa s - is^2, \tag{B10}$$

respectively. We keep the second term on the right-hand side of Eq. (B10) to cover the case where $\kappa \ll 1$. Using Eqs. (B9) and (B10), it is straightforward to obtain the asymptotic formulas

$$I_1(\Lambda) \simeq \pi^{1/2}\Lambda^{-3/2}(i\kappa - 1)^{-1/4} \times \exp\{\tfrac{1}{3}\Lambda^3[3\kappa + 2i + 2(i\kappa - 1)^{3/2}]\}, \tag{B11}$$

$$I_2(\Lambda) = i\Lambda^{-3/2} \int_0^\infty \exp(-\kappa\Lambda^{3/2}s + is^2)ds. \tag{B12}$$

Using the formula

$$(i\kappa - 1)^{1/2} = 2^{-1/2}\{[(1 + \kappa^2) - 1]^{1/2} + i[(1 + \kappa^2) + 1]^{1/2} \operatorname{sign} \kappa\}, \tag{B13}$$

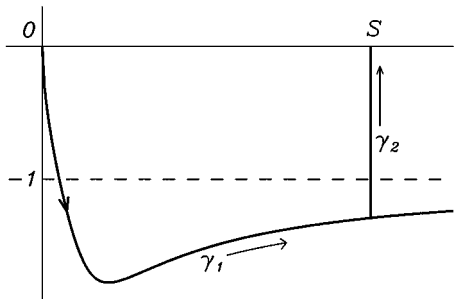

FIG. 6. The picture of the contour of the constant phase γ_1 for $\kappa_c < \kappa < 0$. The contour γ_2 is auxiliary. The dashed line is an asymptote for the contour γ_1. The arrow on the contour γ_1 shows the direction of the steepest descent. The arrows near the contours show the direction of integration.

we obtain

$$\begin{aligned}\Re[3\kappa + 2i + 2(i\kappa - 1)^{3/2}] &= -\kappa^4(4\kappa^2 + 3)[2(\kappa^2 + 1)^{3/2} + 3\kappa^2 + 2]^{-1} \\ &\times \{2^{1/2}|\kappa|[(1 + \kappa^2) + 1]^{1/2} \\ &+ 2^{1/2}[(1 + \kappa^2) - 1]^{1/2} + 3\kappa\}^{-1}.\end{aligned} \tag{B14}$$

It immediately follows from Eq. (B14) that $I_1(\Lambda)$ is exponentially small when $\kappa > 0$ and $\kappa \sim 1$, and can be neglected in comparison with $I_2(\Lambda)$. Hence, we have to retain $I_1(\Lambda)$ in Eq. (B6) only when $\kappa \ll 1$. When $\kappa \ll 1$,

$$3\kappa + 2i + 2(i\kappa - 1)^{3/2} \approx \tfrac{3}{4}i\kappa^2 - \tfrac{1}{8}\kappa^3, \tag{B15}$$

and

$$I_1(\Lambda) \simeq \pi^{1/2}\Lambda^{-3/2} \exp[-\tfrac{1}{4}\pi i + \Lambda^3(\tfrac{1}{4}i\kappa^2 - \tfrac{1}{24}\kappa^3)]. \tag{B16}$$

Finally we obtain

$$F(\sigma;\Lambda) \simeq \pi^{1/2}\Lambda^{-1/2} \exp(-\tfrac{1}{4}\pi i + \tfrac{1}{4}i\sigma^2\Lambda^{-1} - \tfrac{1}{24}\sigma^3\Lambda^{-3}) + i\Lambda^{-1/2} \int_0^\infty \exp(-\sigma\Lambda^{-1/2}s + is^2)ds. \tag{B17}$$

This asymptotic formula is valid for $\sigma > 0$ and $\Lambda \to \infty$.

(ii) $\sigma < 0$. In this case we once again use Eq. (B1) for $F(\sigma;\Lambda)$. However, now the analysis is more complicated because the picture of contours of the stationary phase bifurcates at $\kappa = \kappa_c \equiv -(3 + 2\sqrt{3})^{1/2} \approx -2.542$. Therefore, the asymptotical analysis is different for $\kappa < \kappa_c$ and $\kappa > \kappa_c$.

Let us first study the case where $\kappa < \kappa_c$. In Fig. 6 the contour of the constant phase γ_1 passing through the origin of the coordinates is shown. The horizontal line $\Im(s) = -1$ is an asymptote for this contour as $\Re(s) \to \infty$. The arrow on the contour shows the direction of the steepest descent. Using an auxiliary contour γ_2, we show in the same way as in case (i) that

$$\int_0^\infty \exp[\Lambda^3 h(s)]ds = \int_{\gamma_1} \exp[\Lambda^3 h(s)]ds, \tag{B18}$$

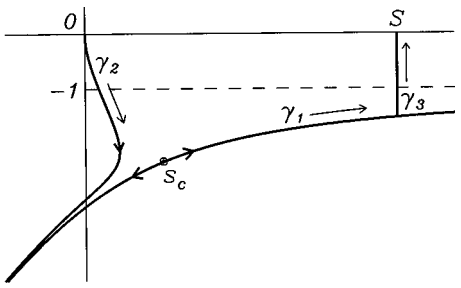

FIG. 7. The same as Fig. 5, however for $\kappa<\kappa_c$.

where the direction of integration along the contour γ_1 is shown by the arrow near the contour. For $\Lambda\to\infty$ the main contribution to the integral on the right-hand side of Eq. (B18) arises from the vicinity of the origin of the coordinates. In this vicinity we can use the approximate expression for the function $h(s)$ given by Eq. (B10). Then, using Eqs. (B1) and Eq. (B18), it is straightforward to obtain

$$F(\sigma;\Lambda)\simeq -i\Lambda^{-1/2}\int_0^\infty \exp(\sigma\Lambda^{-1/2}s+is^2)ds. \qquad \text{(B19)}$$

Let us now proceed to the case where $x<x_c$. In this case the contour of the constant phase passing through the coordinate origin does not have the line $\Im(s)=-1$ as an asymptote. Therefore we have to also use the contour of the constant phase passing through the stationary point s_c determined by Eq. (B3). The two contours are shown in Fig. 7 by the curves γ_2 and γ_1, respectively. The asymptotic analysis is similar to that in case (i). Using the auxiliary contour γ_3, we arrive at Eq. (B6) with $I_1(\Lambda)$ and $I_2(\Lambda)$ determined by Eqs. (B7) and (B8). Once again the main contributions to $I_1(\Lambda)$ and $I_2(\Lambda)$ come from small vicinities of the stationary point s_c and the origin of the coordinates. In the vicinity of s_c the function $h(s)$ can be approximated by Eq. (B9). Since now $|\kappa|\sim 1$, we can use the approximation $h(s)\approx i\kappa s$ in the vicinity of the coordinate origin. These observations enable us to obtain the asymptotic expression

$$I_2(\Lambda)=i\Lambda^{-3}\kappa^{-1} \qquad \text{(B20)}$$

for $I_2(\Lambda)$, and the same asymptotic expression (B11) for $I_1(\Lambda)$. Using Eq. (B3), we obtain

$$\Re[3\kappa+2i+2(i\kappa-1)^{3/2}]$$
$$=3\kappa-2^{-1/2}[(1+\kappa^2)-1]^{1/2}+2^{-1/2}\kappa[(1+\kappa^2)+1]^{1/2}$$
$$<0, \qquad \text{(B21)}$$

so that $I_1(\Lambda)$ is exponentially small as $\Lambda\to\infty$ and can be neglected in comparison with $I_2(\Lambda)$. As a result we obtain $F(\sigma;\Lambda)\simeq -i\sigma^{-1}$. Since this asymptotic expression follows from Eq. (B19) when $|\sigma|\gtrsim\Lambda^{1/2}$ ($|\kappa|\gtrsim\Lambda^{-3/2}$), we conclude that asymptotics (B19) is uniformly valid for $\sigma<0$, $|\sigma|\lesssim\Lambda^2$ ($|\kappa|\lesssim 1$).

Asymptotic formulas (B17) and (B19) are uniformly valid in a very wide interval of variation of σ, namely for $|\sigma|\lesssim\Lambda^2$. However, these formulas are relatively complicated because they contain integrals. Narrowing the interval of the variation of σ results in simplification of these asymptotic formulas. First, we consider the interval $|\sigma|\ll\Lambda^{1/2}$. In this interval the both formulas are reduced to

$$F(\sigma;\Lambda)\simeq \tfrac{1}{2}\pi^{1/2}\Lambda^{-1/2}e^{-\pi i/4}-\sigma\Lambda^{-1}. \qquad \text{(B22)}$$

Hence, in spite that Eq. (B17) was derived for $\sigma>0$, and Eq. (B19) for $\sigma<0$, both asymptotic expressions are valid in the overlap region $|\sigma|\ll\Lambda^{1/2}$.

The other interesting case is $\sigma<0$, $|\sigma|\gg\Lambda^{1/2}$. In this case it immediately follows from Eq. (B19) that

$$F(\sigma;\Lambda)\simeq i\sigma^{-1}. \qquad \text{(B23)}$$

We obtain the same asymptotic behavior for large positive values of σ, however now it is valid only when the first term on the right-hand side of Eq. (B17) is small comparing with the second one, i.e., when $|\sigma|\gg\Lambda$. The asymptotic formula (B23) coincides with Eq. (A1) describing the asymptotic behavior of $F(\sigma;\Lambda)$ as $|\sigma|\to\infty$. We see that for large Λ this asymptotic behavior takes place when $|\sigma|\gg\Lambda^{1/2}$ for $\sigma<0$; however, for $\sigma>0$ it takes place only when $|\sigma|\gg\Lambda$. It can be shown that the same is true for the asymptotic behavior of $G(\sigma;\Lambda)$ as $|\sigma|\to\infty$, given by Eq. (A10).

It is also instructive to describe the behavior of the function $F(\sigma;\Lambda)$ for $\Lambda^{1/2}\lesssim\sigma\lesssim\Lambda$. It can be seen from Eq. (B17) that in this interval the function $F(\sigma;\Lambda)$ oscillates with the period of the order $\Lambda^{1/2}$ and decays with the characteristic scale Λ.

[1] L. Chen and A. Hasegawa, J. Geophys. Res. **79**, 1024 (1974).
[2] D. J. Southwood, Planet. Space Sci. **22**, 483 (1974).
[3] W. J. Hughes, *Solar Wind Sources of Magnetospheric Ultra-Low-Frequency Waves*, edited by M. J. Engebretson, K. Takahashi, and M. Scholer, Geophysical Monograph 81 (American Geophysical Union, Washington, 1994), p. 1.
[4] A. N. Wright, *Physical Signatures of Magnetospheric Boundary Layer Processes*, edited by J. A. Holtet and A. Egeland (Kluwer, Netherlands, 1994), p. 329.
[5] J. A. Ionson, Astrophys. J. **226**, 650 (1978).
[6] M. Kuperus, J. A. Ionson, and D. Spicer, Annu. Rev. Astron. Astrophys. **19**, 7 (1981).
[7] J. A. Ionson, Sol. Phys. **100**, 289 (1985).
[8] J. M. Davila, Astrophys. J. **317**, 514 (1987).
[9] J. V. Hollweg, *Mechanism of Chromospheric and Coronal Heating*, edited by P. Ulmschneider, E. R. Priest, and R. Rosner (Springer-Verlag, Berlin, 1991), p. 423.
[10] M. Goossens, *Advances in Solar System Magnetohydrodynamics*, edited by E. R. Priest and A. W. Hood (Cambridge U. P., Cambridge, 1991), p. 135.
[11] J. V. Hollweg, Astrophys. J. **335**, 1005 (1988).
[12] Y.-Q. Lou, Astrophys. J. **350**, 452 (1990).
[13] T. Sakurai, M. Goossens, and J. V. Hollweg, Sol. Phys. **133**, 247 (1991).
[14] M. Goossens and S. Poedts, Astrophys. J. **384**, 348 (1992).
[15] M. Goossens and J. V. Hollweg, Sol. Phys. **145**, 19 (1993).
[16] H. Stenuit, S. Poedts, and M. Goossens, Sol. Phys. **147**, 13 (1993).
[17] A. N. Wright and M. J. Thompson, Phys. Plasmas **1**, 691 (1994).
[18] S. J. Schwartz and N. Bel, Sol. Phys. **92**, 133 (1984).
[19] M. Goossens, S. Poedts, and D. Hermans, Sol. Phys. **102**, 51 (1985).
[20] P. J. Hansen and B. G. Harrold, J. Geophys. Res. **99**, 2429 (1994).
[21] A. N. Wright and A. R. Garman, J. Geophys. Res. **103**, 2377 (1998).
[22] M. S. Ruderman, W. Tirry, and M. Goossens, J. Plasma Phys. **54**, 129 (1995).
[23] W. Tirry and M. Goossens, Astrophys. J. **471**, 501 (1996).
[24] J. P. Boris, ''Resistive modified normal modes of an inhomogeneous incompressible plasma,'' Ph.D. thesis, Princeton University, UMI Dissertation Services, Ann Arbor Michigan, 1968, p. 172.

[25]Y. Mok and G. Einaudi, J. Plasma Phys. **33**, 199 (1985).
[26]M. Goossens, M. S. Ruderman, and J. V. Hollweg, Sol. Phys. **157**, 75 (1995).
[27]M. Goossens and M. S. Ruderman, Phys. Scr. **T60**, 171 (1995).
[28]T. Sakurai, M. Goossens, and J. V. Hollweg, Sol. Phys. **133**, 227 (1991).
[29]A. N. Wright and W. Allan, J. Geophys. Res. **101**, 17,399 (1996).
[30]A. N. Nayfeh, *Introduction to Perturbation Techniques* (Wiley-Interscience, New York, 1981).
[31]C. M. Bender and S. A. Orszag, *Advanced Mathematical Methods for Scientists and Engineers* (McGraw-Hill, Auckland, 1987).